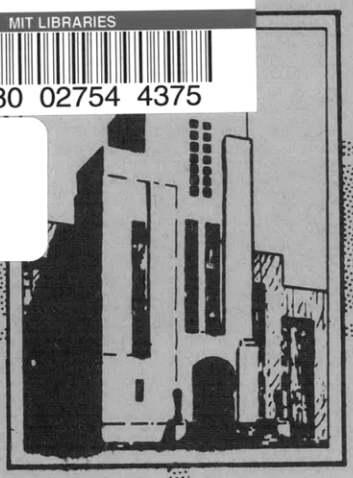

DEPARTMENT OF THE NAVY

DAVID TAYLOR MODEL BASIN

HYDROMECHANICS

AERODYNAMICS

STRUCTURAL MECHANICS

APPLIED MATHEMATICS

EXPERIMENTAL DETERMINATION OF THE FORCES ON SUPERCAVITATING HYDROFOILS WITH INTERNAL VENTILATION

by

N.L. Ficken, Jr. and G.F. Dobay

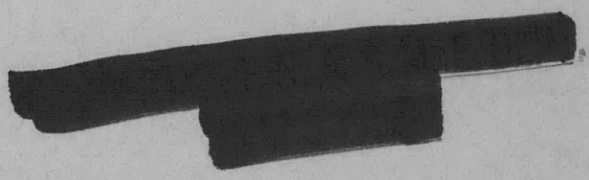

HYDROMECHANICS LABORATORY

RESEARCH AND DEVELOPMENT REPORT

January 1963

Report 1676

EXPERIMENTAL DETERMINATION OF THE FORCES ON SUPERCAVITATING HYDROFOILS WITH INTERNAL VENTILATION

by

N.L. Ficken, Jr. and G.F. Dobay

January 1963

Report 1676
S-F013 02 01

TABLE OF CONTENTS

LIST OF FIGURES

NOTATION

A_p Vertical projected area of the hydrofoil, sq ft

C_D Drag coefficient, $D/\frac{\rho}{2} scv^2$

C_{Dm} Measured drag coefficient, $D_m/\frac{\rho}{2} scv^2$

C_{Ds} Strut drag coefficient $D_s/\frac{\rho}{2} cv^2$

C_L Lift coefficient, $L/\frac{\rho}{2} scv^2$

$C_{L,d}$ Design lift coefficient

C_{Lo} Lift coefficient for zero cavitation number

c Chord of the hydrofoil, ft

D Drag, lb

D_m Drag of the hydrofoil-strut combination, lb

D_s Strut drag, lb

d Depth of immersion, in.

K_v Ventilation index, Q/VA_p

L Lift, lb

p_c Pressure in the cavity, lb/sq ft

p_m Measured pressure at the Flowrator, psia

p_v Vapor pressure, lb/sq ft

p_∞ Free-stream static pressure, lb/sq ft

Q Ventilating air-flow rate, corrected to atmospheric pressure, cu ft/min

Q_m Measured ventilating air-flow rate, cu ft/min

q_∞ Free-stream dynamic pressure, $\rho v^2/2$, lb/sq ft

s Span of the hydrofoil, ft

V Speed, ft/min

v Speed, ft/sec

α Angle of attack, deg

ρ Density, lb-sec^2/ ft^4

σ Cavitation number, $\dfrac{p_\infty - p_c}{q_\infty}$

σ_c Cavitation number based on measured cavity pressure, $\dfrac{p_\infty - p_c}{q_\infty}$

σ_{nv} Effective cavitation number for nonventilated hydrofoil

σ_v Cavitation number based on vapor pressure, $\dfrac{p_\infty - p_v}{q_\infty}$

ABSTRACT

The design of supercavitating propellers and high-speed supercavitating hydrofoil craft requires that the lift and drag characteristics of supercavitating foils be known for cavitation numbers approaching zero. Since many test facilities cannot achieve the high speeds associated with near-zero cavitation number, an investigation is in progress at the Taylor Model Basin to develop techniques for using internal ventilation to produce very low cavitation numbers at low and moderate speeds. A nondimensional coefficient, the ventilation index K_v, has been defined. It has been found that the cavitation number based on measured cavity pressure behaves differently for ventilated flows at speeds in the supercavitating regime and at speeds in the subcavitating regime. In both cases, however, the measured cavitation number is related directly to the ventilation index and is relatively insensitive to angle of attack. At high values of the ventilation index (about 0.19 for tests of the 5-term foil reported here), the lift and drag coefficients become constant at values appropriate to zero cavitation number. Methods for relating the lift and drag coefficients for various ventilating airflow rates to the appropriate cavitation number are presented for the two speed ranges. Discrepancies exist between the results obtained from high- and low-speed ventilated tests. Further investigation will be required to refine the procedures.

INTRODUCTION

The lift and drag coefficients of supercavitating hydrofoils depend both on angle of attack and cavitation number. Cavitation number may in general be defined as

$$\sigma = \frac{p_\infty - p_c}{q_\infty}$$

where p_∞ is the free-stream static pressure,

p_c is the pressure in the cavity, and

$q_\infty = \frac{\rho}{2} v^2$ is the free-stream dynamic pressure.

In supercavitating flow, defined here as having a vapor-filled cavity, the cavity pressure is generally assumed equal to the vapor pressure p_v.

In a towing basin or other facility with atmospheric pressure at the water surface, only a small variation in p_∞ can be achieved by varying depth. Accordingly, tests must be conducted at very nearly the speed of the prototype to satisfy $\sigma_m = \sigma_p$. Since speeds up to 100

knots are under consideration, and probably higher speeds in the future, many facilities through the country, including the high-speed basin, at the Taylor Model Basin are inadequate for this type of test.

In a variable-pressure water tunnel, the static pressure can be reduced considerably. The reduction is limited, however, since there must be a head of water above the hydrofoil, and the pressure above the water surface must be greater than vapor pressure to avoid boiling of the tunnel water. At the highest speed available in the 24-in. diameter water tunnel at the Model Basin for example, the minimum cavitation number obtainable is 0.1. This is higher than the cavitation number of 0.075 which would occur on a 100-knot hydrofoil boat. In addition, if section data are to be obtained for the design of supercavitating propellers, even lower cavitation numbers must be considered.

Ventilated flows, defined here as having a cavity filled with air (or another gas if desired) which can exist in equilibrium with water at pressures higher than vapor pressure, are being investigated at the Model Basin as a possible means of extending the C_L, C_D versus σ relations to zero cavitation number. Two types of ventilation may be considered: (1) natural or surface ventilation, where the main cavity or the hydrofoil tip vortex cavities are open to the atmosphere through the water surface and (2) internal or forced ventilation, where air is blown into the cavity through the back (suction side) of the foil. The Model Basin investigation deals with internal ventilation and determination of the means for interpreting the measurements of lift and drag obtained with various combinations of speed and airflow in terms of C_L and C_D versus σ. This paper presents the current progress of this investigation.

MODEL CONFIGURATION

Tests were conducted with a three-dimensional "Johnson 5-term"[1] hydrofoil with aspect ratio 3 rectangular planform. The shape of the face (pressure side) was designed for a design lift coefficient of $C_{L,d} = 0.1964$ at zero angle of attack with respect to the X-reference axis. The dimensions of the foil are shown in Figure 1. This foil was selected because tests had previously been run to near-zero cavitation number at the National Aeronautics and Space Administration.[2] To be consistent with previous Model Basin work in this area, angles of attack in this paper are referred to the nose-tail line of the foil, which is at an angle of 1.88 degrees with respect to the X-axis shown in Figure 1 and in References 1 and 2. The foil was supported on a single strut with NACA 66, 1-012 section. The dimensions of the strut are shown in Figure 2. The strut was mounted perpendicular to the back surface of the foil in the center of the span. No fillets were used at the intersection.

To accommodate the flow of ventilating air to the cavity, slots were machined in the back surface of the foil. Cover plates were soldered in place over the slots and drilled as shown in Figure 3. The slots connected with a vertical 3/16-in. diameter hole in the strut.

[1]References are listed on page 19.

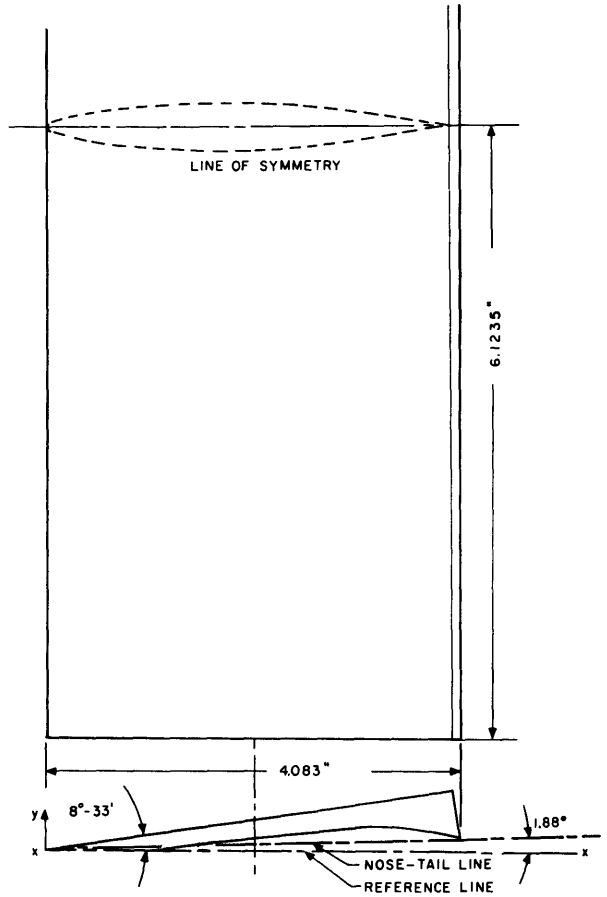

Table of Coordinates for Lower Surface

x	y
in.	in.
0	0
0.102	0.002
0.204	0.004
0.408	0.009
0.817	0.024
1.225	0.044
1.429	0.068
1.633	0.075
1.837	0.096
2.041	0.117
2.245	0.142
2.450	0.168
2.654	0.194
2.858	0.218
3.062	0.234
3.266	0.243
3.355	0.244
3.470	0.243
3.674	0.227
3.878	0.198
4.083	0.134

Figure 1 – Hydrofoil Model Dimensions

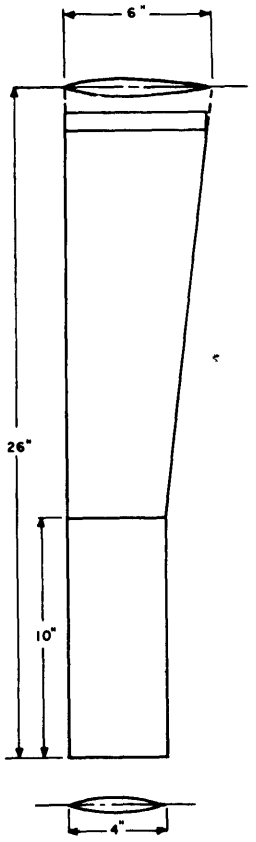

Hydrofoil Towing Strut
DTMB – 10/31/60

Strut Section Offsets (NACA 66,1-012)

x/c	y/c
L.E.	0
.0050	.00900
.0075	.01083
.0125	.01343
.025	.01803
.050	.02484
.075	.03019
.10	.03482
.15	.04214
.20	.04779
.25	.05218
.30	.05550
.35	.05786
.40	.05934
.45	.05998
.50	.05972
.55	.05844
.60	.05594
.65	.05165
.70	.04535
.75	.03789
.80	.02964
.85	.02098
.90	.01244
.95	.00477
1.00	0

Figure 2 – Strut Dimensions

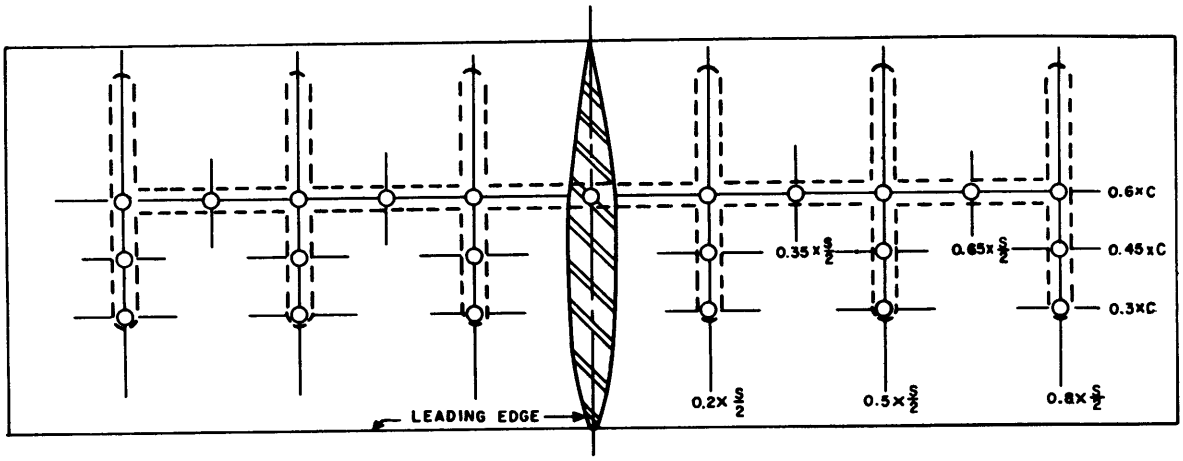

Figure 3 – Layout of Ventilation Holes

TEST APPARATUS

The tests were conducted at the Model Basin on the high-speed towing carriage (Carriage No. 5). The supporting strut was attached to the lift-drag dynamometer shown in Figure 4. Lift and drag were measured by six TMB differential reluctance modular-force gages mounted in a triangular array as shown in Figure 5. Three two-channel TMB control units, Model 302-1A, were used in conjunction with six Dynametrics Model 416 digital strain-gage indicators, modified for this purpose, to obtain direct numerical reading of the gage outputs. In order to preserve the readings during deceleration of the towing carriage, input to the digital servomotors was switched off when a steady-state condition was reached. Calibration of the hydrofoil dynamometer showed a consistent interaction between pitch moment and lift. The lift measurements were corrected for this effect. There was no interaction effect on the drag measurements.

Internal ventilation was accomplished in the manner indicated schematically in Figure 6. Bottled compressed air was supplied to the system via a low-pressure (200 psig) reservoir and metered by a Fisher-Porter "Flowrator." A pressure gage was located at the Flowrator to allow correction of the airflow readings to standard conditions. The correction used, which was based on the characteristics of the Flowrator, is

$$Q = Q_m \sqrt{\frac{p_m}{14.7}}$$

where Q_m is the measured volume rate of flow in cubic feet per minute ,

Q is the volume rate of flow of equivalent mass of air at atmospheric pressure in cubic feet per minute, and

p_m is the measured pressure at Flowrator in pounds per square in. absolute.

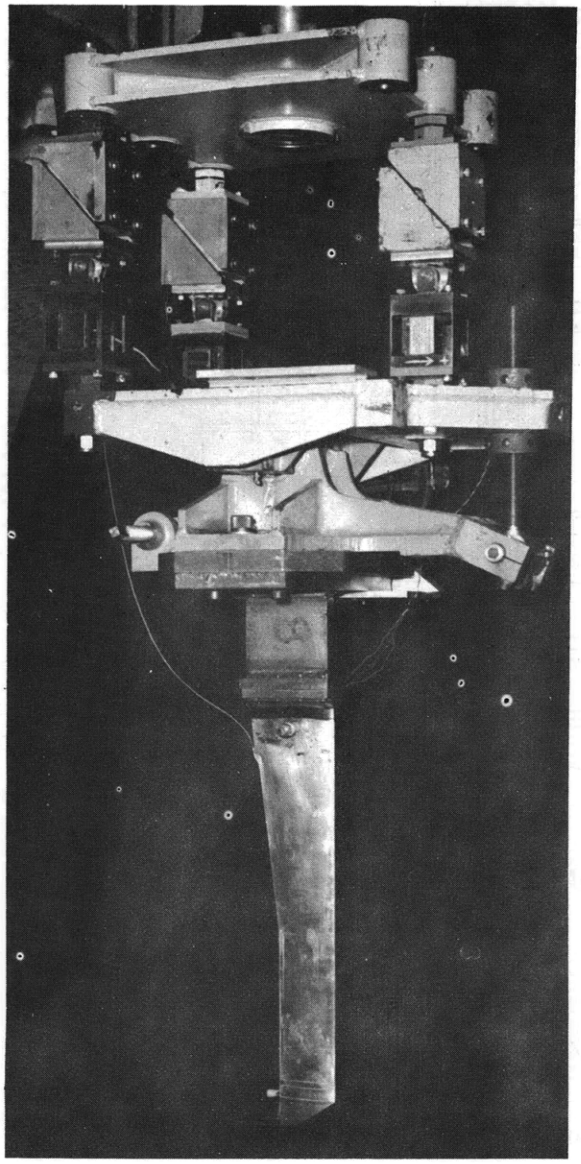

Figure 4 – Hydrofoil Dynamometer

Cavity pressure was measured by a 0- to 50-psia Micro-Systems Type P03BA5 semiconductor pressure transducer. The transducer had a 1/4-in.-diameter diaphragm and was mounted in a 1/2-in.-diameter probe extending 1-1/16 in. from the trailing edge of the foil as shown in Figure 7. The transducer was driven at 2 v.d.c. and its output voltage converted to an a-c voltage with frequency proportional to the voltage by a Vidar Model 240AR voltage-to-frequency converter. The frequency was measured and recorded by a Hewlett-Packard Model 522B Electronic Counter and associated printer.

TEST PROCEDURE

All tests were conducted under steady-state conditions; i.e., no change was made in angle of attack, depth, speed, or airflow rate during any test run. After a steady speed had been achieved, speed, lift, drag, cavity pressure, and airflow rate were measured during each run. The lift measurements were corrected for the pitch moment interaction effect mentioned earlier, and lift and drag coefficients were computed by:

$$C_L = \frac{L}{\frac{\rho}{2} scv^2}$$

$$C_D = \frac{D}{\frac{\rho}{2} scv^2}$$

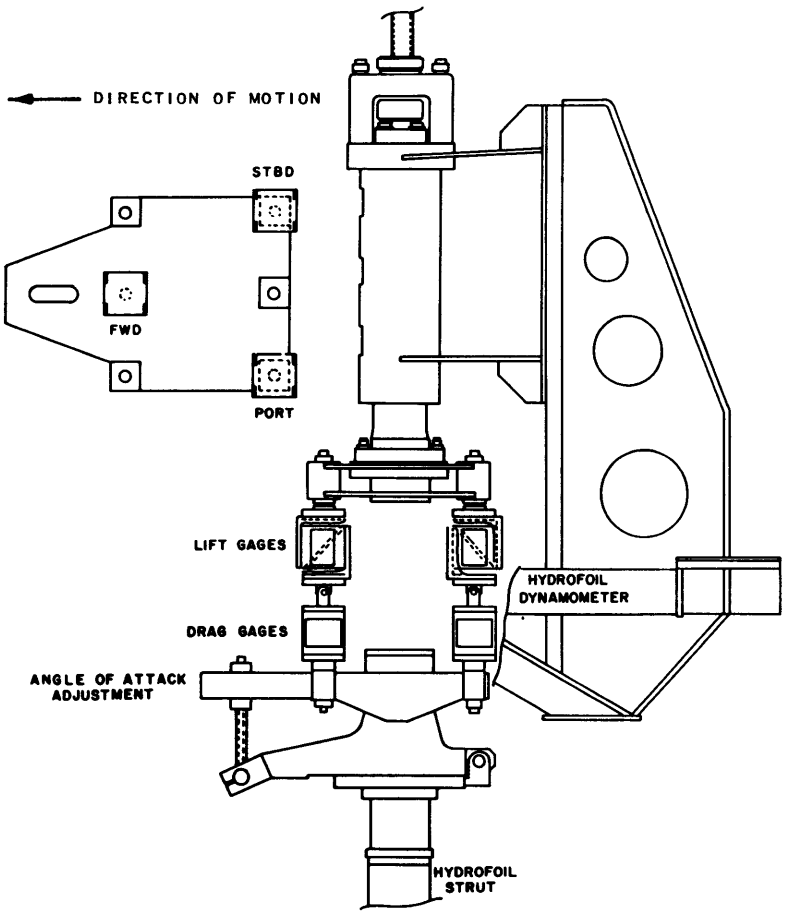

Figure 5 – Arrangement of Lift and Drag Gages

where L is the lift in pounds,

D is the drag in pounds,

ρ is the density of the water in lb-sec^2/ft^4,

s is the span of the hydrofoil in feet,

c is the chord of the hydrofoil in feet, and

v is the speed in feet per second.

In order to obtain the drag of the hydrofoil alone, the drag coefficient of the strut was subtracted from the measured drag coefficient. To determine the strut drag, the strut was towed at several depths and angles of attack. It was found that the strut-drag coefficient was independent of speed for Froude number greater than 2.0, indicating that the surface drag of the strut was negligible. The strut-drag coefficient was also found to be relatively independent of angle of attack. Plotting the strut-drag coefficient against depth of immersion yielded the linear relation

$$C_{Ds} = 0.0014 + 0.0084\ d$$

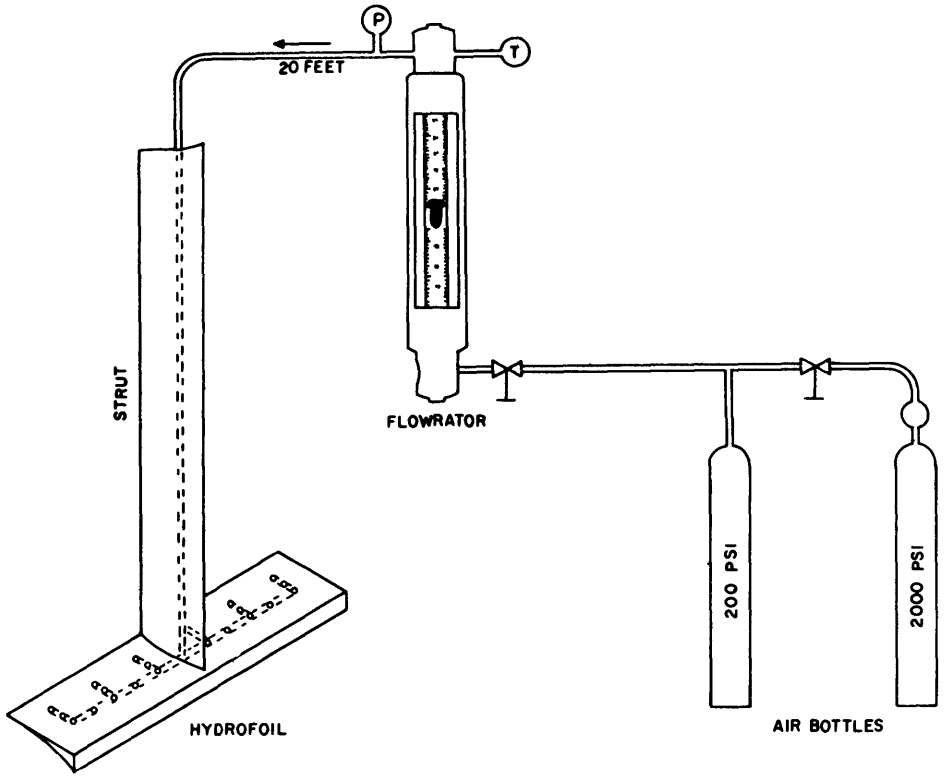

Figure 6 – Ventilation System

where C_{Ds} is the strut drag coefficient and

d is the depth in feet.

It was assumed that the first term represented the drag of the tip of the strut. Since the tip was not exposed when supporting the foil, this term was removed. The correction applied to the measured drag coefficients was thus

$$C_D = C_{Dm} - 0.0084 \frac{d}{s}$$

The interaction effect between strut and foil was considered negligible since in supercavitating or ventilated condition, the intersection is enclosed by the cavity.

The cavitation number, based on measured cavity pressure, is

$$\sigma_c = \frac{p_\infty - p_c}{q_\infty}$$

Before and after each test run, a static pressure reading was obtained. Since the gage was mounted on the foil, this reading represented the absolute ambient pressure p_∞. During each run, the cavity pressure p_c was measured.

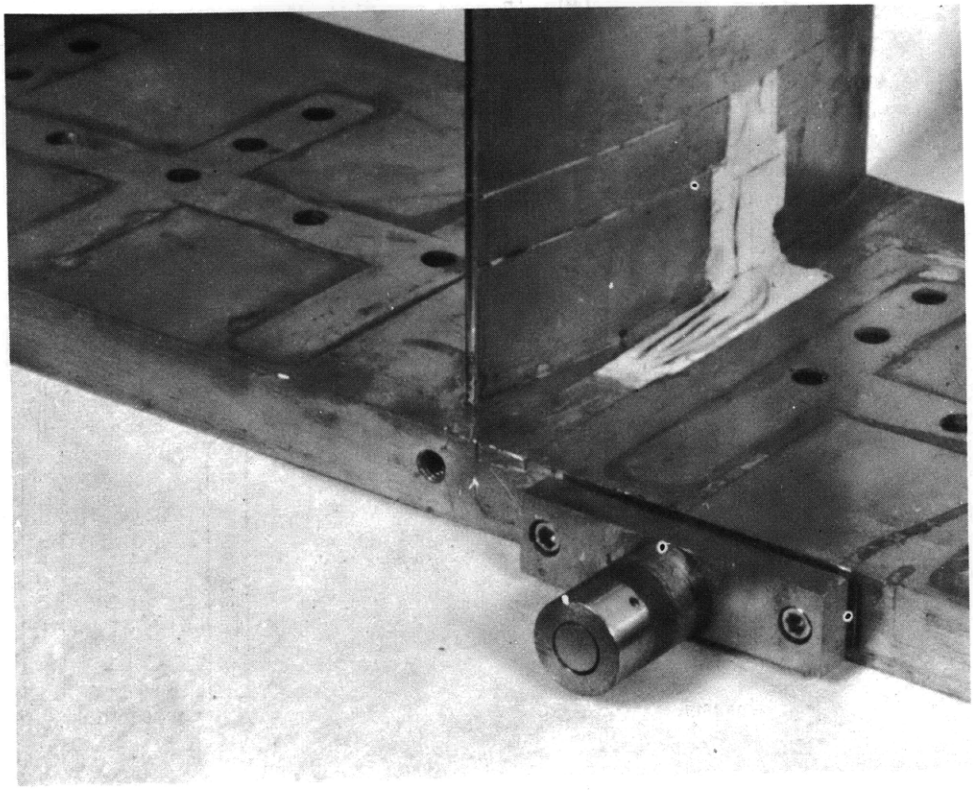

Figure 7 – Cavity Pressure Gage Installation

As mentioned earlier, the airflow measurements were corrected to atmospheric pressure. A nondimensional ratio designated ventilation index K_v is defined as

$$K_v = \frac{Q}{VA_p}$$

where Q is the volume rate of airflow adjusted to atmospheric pressure in cubic feet per minute,

V is the speed in feet per minute, and

A_p is the projected area of the foil perpendicular to the direction of motion in square feet.

For a given angle of attack, K_v can be varied by changing either the airflow rate or the speed. A_p is a function of angle of attack and for angles in excess of 6.4 deg is

$$A_p = cs \sin\alpha$$

The tests reported here were conducted at angles of attack of 11, 12, and 14 deg. Ventilated and nonventilated tests were run at speeds from 15 to 50 knots. A minimum angle of 11 deg was used because a fully developed cavity could not be achieved consistently at

lower angles. That difficulty in obtaining a full cavity below 11 deg should occur is confirmed by the data of Reference 2. A portion of these data have been plotted in Figure 8; they were obtained from high-speed tests at the Langley tank and correspond to very low cavitation numbers (of the order of 0.005). At angles of attack less than 11 deg, C_L rises above the straight-line relation which would be expected, indicating that the foil was only partially cavitated. The curve bends down and approaches the subcavitating curve below 6-deg angle of attack.

ANALYSIS OF RESULTS

CAVITATION NUMBER

When the hydrofoil was tested without ventilation at speeds sufficient to supercavitate, the cavitation number σ_c calculated using the measured cavity pressure was found to be generally lower than the cavitation number σ_v obtained using the vapor pressure appropriate to the ambient temperature. A typical plot of these measurements obtained in tests in the towing basin is shown in Figure 9. As the cavitation number was decreased, the measured cavitation number reached a constant limiting percentage of the vapor cavitation number, in this case about 93 percent. Increase of cavitation number produced a drop in the ratio σ_c/σ_v starting at about $\sigma_v = 0.5$ as the pressure gage approached the increasing cavity pressure at the rear of the cavity and beyond.[3] Similar results have been obtained by other researchers.[4] No explanation for the discrepancy between the measured cavity pressure and vapor pressure will be attempted at this time. However, instrumentation is under construction for measuring the drag and cavity pressure of supercavitating plates and disks in the towing basin and water tunnels, and a more extensive investigation of this question will be made in the future. For the present, the limiting value of the cavity pressure has been used in place of the vapor pressure to calculate an effective cavitation number σ_{nv} which is used for the remainder of the analysis.

Analysis of the ventilated tests must be separated into two categories depending on the speed: (1) high speed, sufficient to supercavitate without ventilation and (2) low speed, in the subcavitating range when the foil is not ventilated. A third speed range, in which the foil would be partially cavitated without ventilation, will not be considered at this time because insufficient data are available to evaluate the behavior which is somewhere between that of the other two ranges.

The basic difference between high-speed and low-speed ventilation is shown by the measured cavitation number. As shown in Figure 10, for high-speed ventilation, the ratio σ_c/σ_{nv} is a function of K_v only. Similar curves were also presented in Reference 5. Since by definition, $\sigma_c = \sigma_{nv}$ for the nonventilated foil in this speed range, the ratio σ_c/σ_{nv} is unity at $K_v = 0$. The treatment of the lower end of the curve will be discussed later in connection with lift and drag.

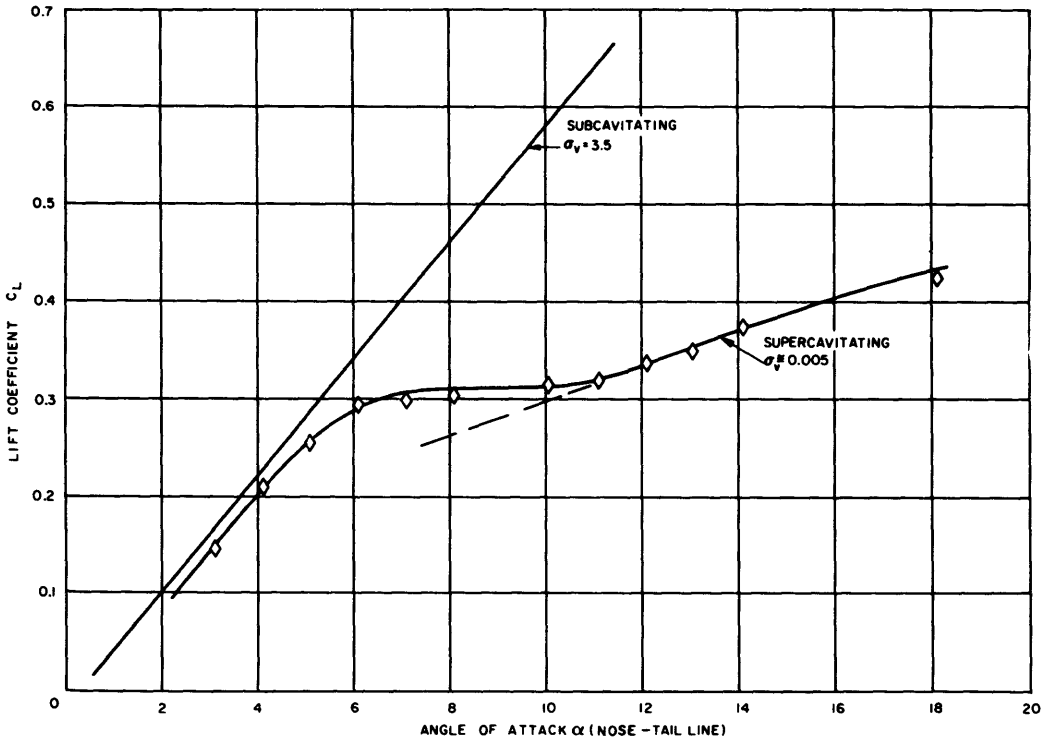

Figure 8 – Variation of Lift Coefficient with Angle of Attack for Near-Zero Cavitation Number

(obtained from Reference 2)

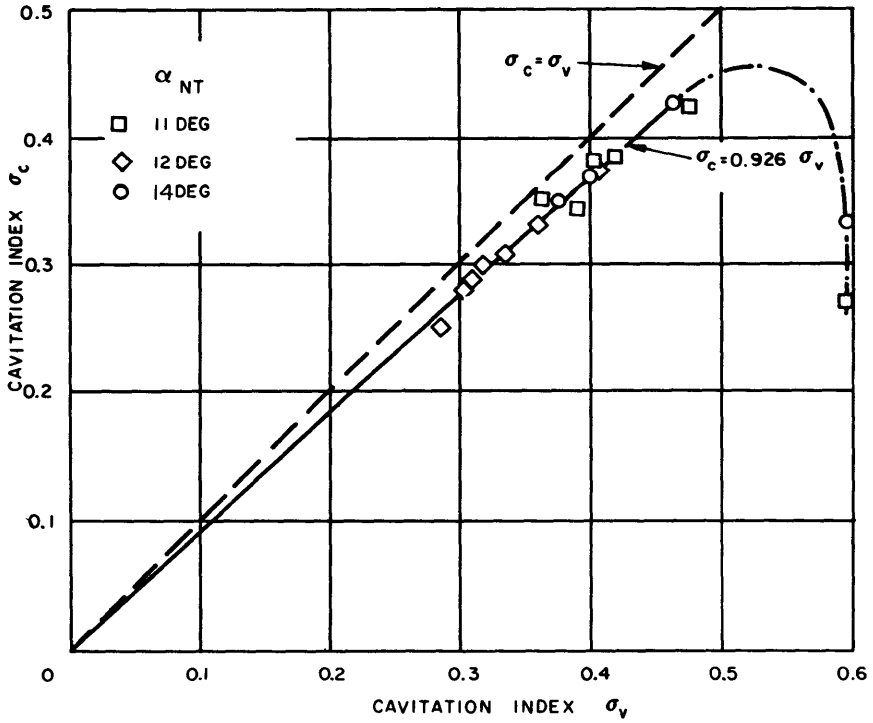

Figure 9 – Comparison of Cavitation Number Based on Measured Cavity Pressure and Cavitation Number Based on Vapor Pressure for the Nonventilated Hydrofoil

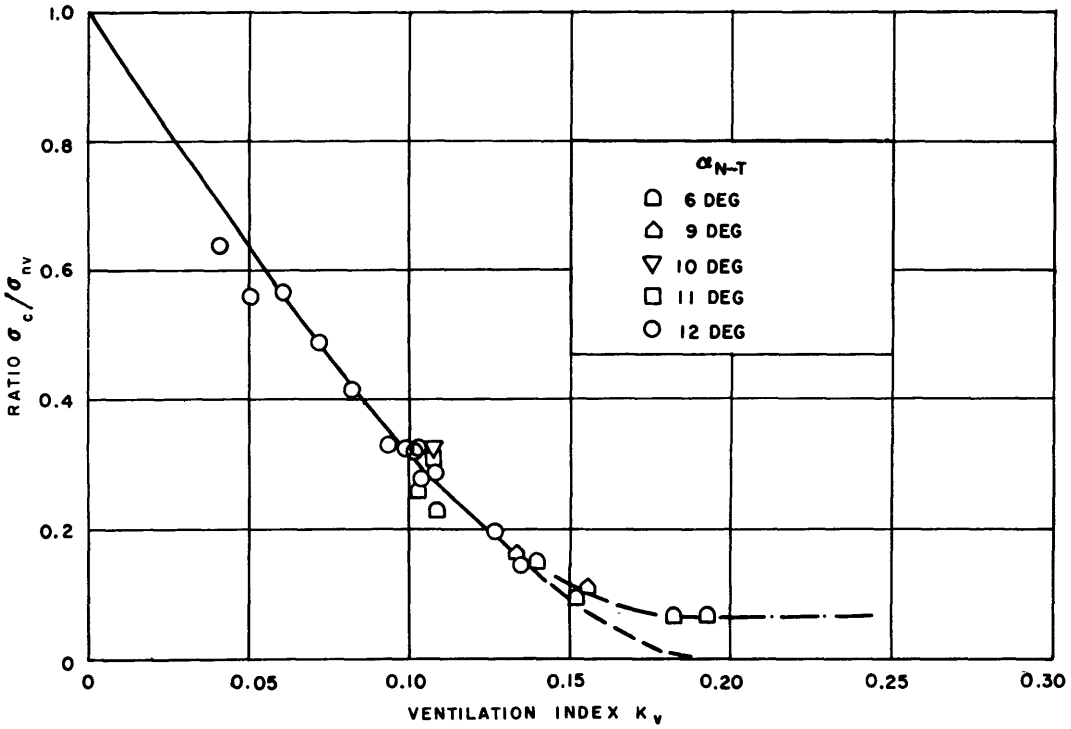

Figure 10 – Variation of the Ratio σ_c/σ_{nv} with Ventilation Index for the Ventilated Hydrofoil at Supercavitating Speeds

The ratio σ_c/σ_{nv} has no significance for low-speed ventilation. Instead, as shown in Figure 11, the measured cavitation number σ_c is generally independent of speed and depends only on ventilation index K_v. As mentioned previously, σ_c is not considered to be a true measure for high cavitation numbers. Thus in drawing a curve of effective cavitation number for low-speed ventilation, the measured σ_c as $K_v \to 0$ must be ignored. Instead, the curve must intersect the $K_v = 0$ line at the value of the vapor cavitation number σ_{nv}. The curve is shown dotted in this region because the shape is not definitely known. Values in this region are not used to obtain the final results. Determination of the path of the curve and treatment of the lower end will be discussed in connection with lift and drag.

LIFT AND DRAG

For the nonventilated tests, the circles on Figures 12 and 13 represent the lift and drag coefficients plotted against the effective cavitation number σ_{nv}. The shape of these curves is typical for supercavitating foils. As the cavitation number is reduced from the subcavitating regime, the lift and drag rise as partial cavitation occurs. This rise occurs earlier for drag because the base, or trailing edge, starts to cavitate earlier than the back and the base cavity, for low or moderate angles of attack, has very little effect on lift. When

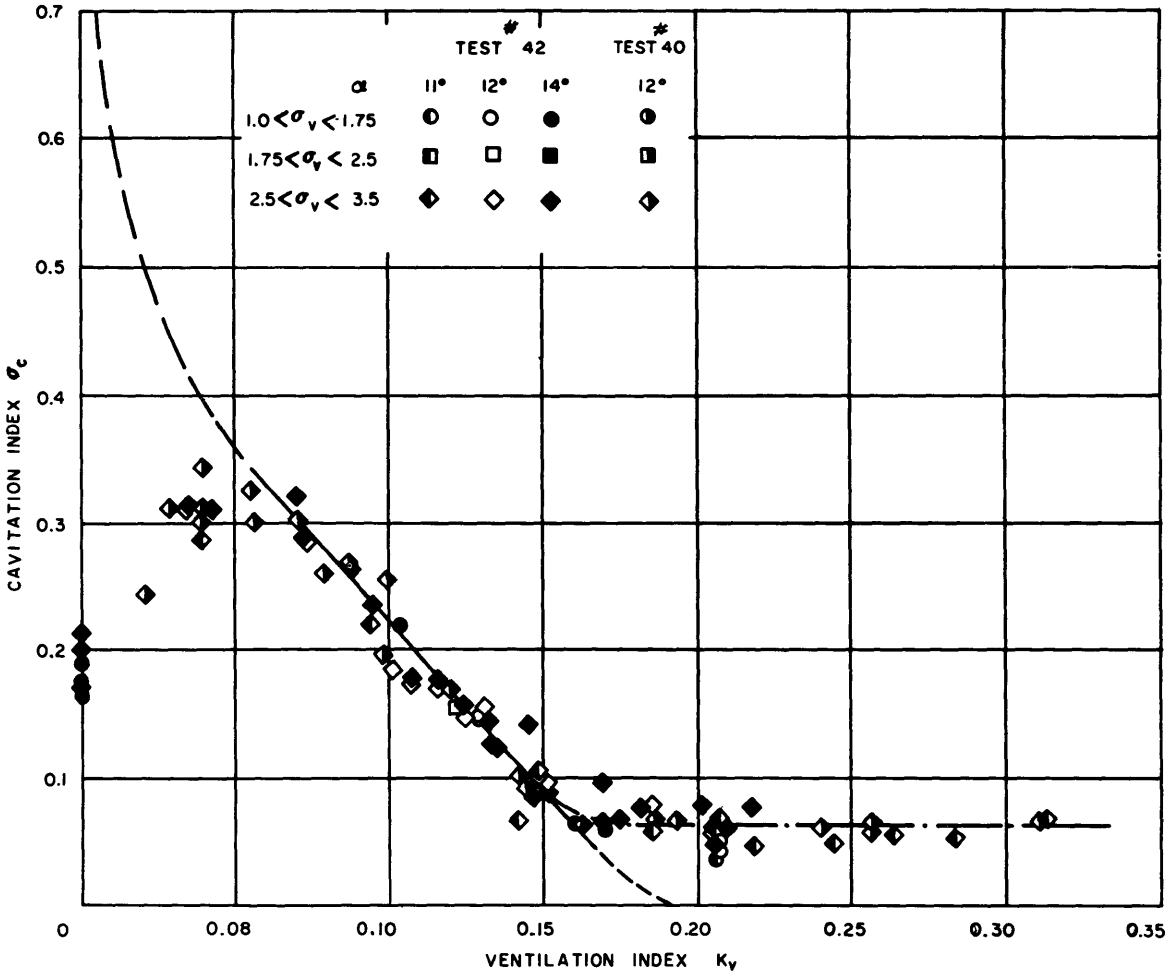

Figure 11 – Variation of Cavitation Number Based on Measured Cavity Pressure for the Ventilated Hydrofoil at Subcavitating Speeds

the foil is supercavitating, i.e., the cavity is fully formed, the lift and drag decrease for further decrease in cavitation number.

The dashed lines on Figures 12 and 13 represent the results obtained by ventilating at subcavitating speeds. To obtain these curves, C_L and C_D were plotted against K_v as shown in Figure 14. As in the case of σ_c discussed earlier, C_L and C_D were generally independent of speed and a single curve could be drawn at a given angle of attack. Values of C_L from Reference 2 plotted on Figure 8 are shown on Figure 14 as C_{L_o}. As mentioned previously, these values represent very nearly zero cavitation number and are treated as occurring at essentially zero cavitation number. It was not possible to use the C_D values from Reference 2 because data were not available for evaluating the strut drag. It was found that C_L leveled off at values equal to C_{L_o} for values of the ventilation index in excess of 0.19. This range ($K_v > 0.19$) is designated the range of full ventilation. The measured

Figure 12 – Variation of Lift Coefficient with Cavitation Number

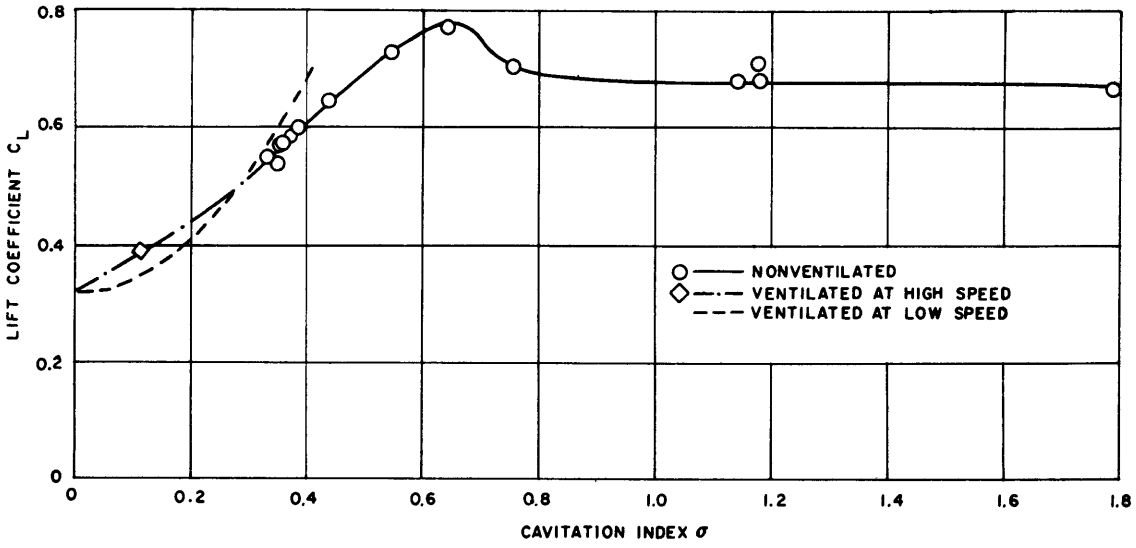

Figure 12a – 11-Degree Angle of Attack

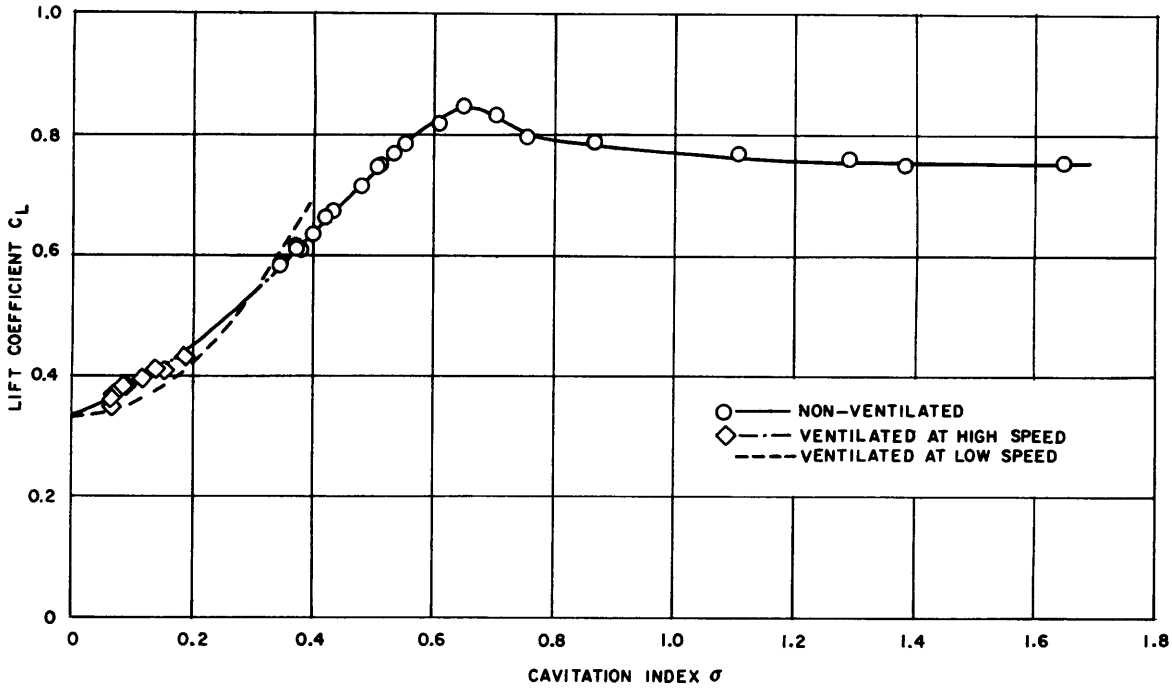

Figure 12b – 12-Degree Angle of Attack

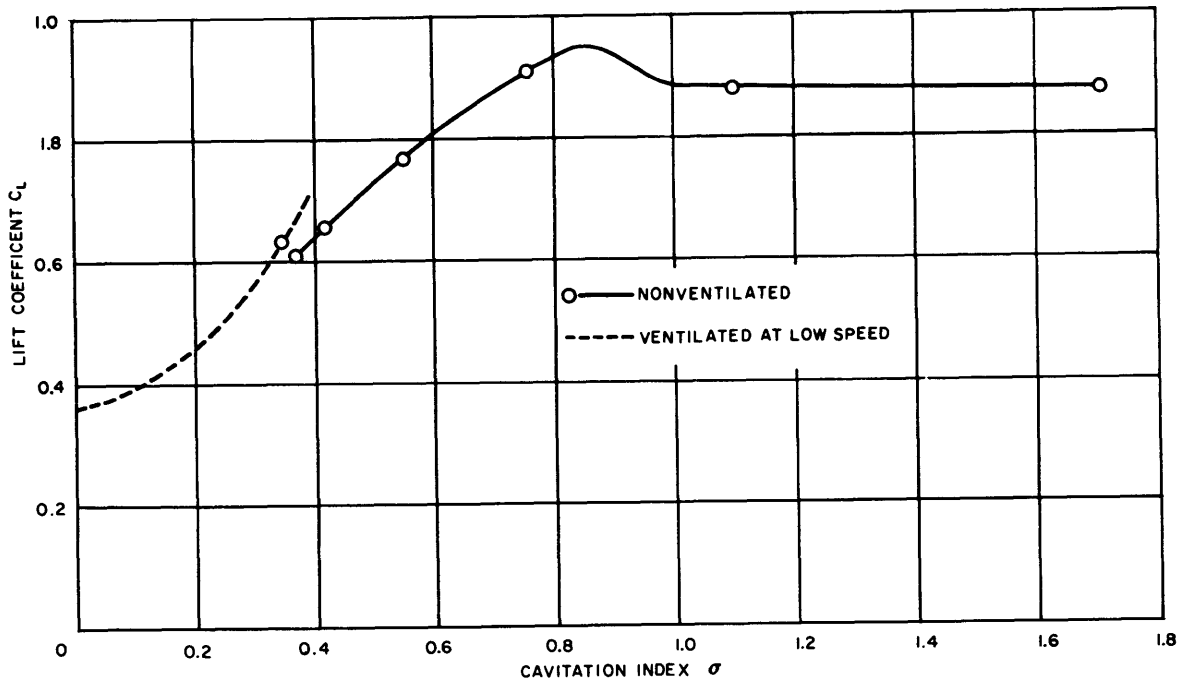

Figure 12c – 14-Degree Angle of Attack

values of σ_c, on the other hand, leveled off at values considerably above zero. The reason has not yet been determined, but based on these measurements and on measurements made with other hydrofoils using another pressure gage which gave valid results for only high K_v, it appears that the cavity pressure is limited to a maximum value equal to the atmospheric pressure. Zero cavitation number requires that the cavity pressure equal the atmospheric pressure plus the head of water above the foil. Leaving this question unanswered for the present, it was assumed that the foil was operating at effectively zero cavitation number for values of K_v greater than 0.19. Accordingly, the curve of σ_c versus K_v on Figure 11 was faired to a value of $\sigma = 0$ at $K_v = 0.19$. Since σ_c is not considered adequately defined below $K_v = 0.05$, it is not required to know the shape of C_L and C_D curves below this value of K_v. The curves have been extended, however, to indicate the expected general shape. It is expected that these curves should have a peak corresponding in magnitude to the peaks obtained in nonventilated operation. Unfortunately, it was not possible to control the very small quantity of air required to define the peak. If this could have been done, the value of K_v at which the peak occurred could have been related to the value of σ_{nv} at which the nonventilated peak occurred, thus permitting definition of the σ_c versus K_v curve for almost the entire range of K_v.

The diamond-shaped symbols of Figures 12a, 12b, 13a, and 13b represent the results of the high-speed ventilated tests. Here the measured lift and drag coefficients were plotted

Figure 13 – Variation of Drag Coefficient with Cavitation Number

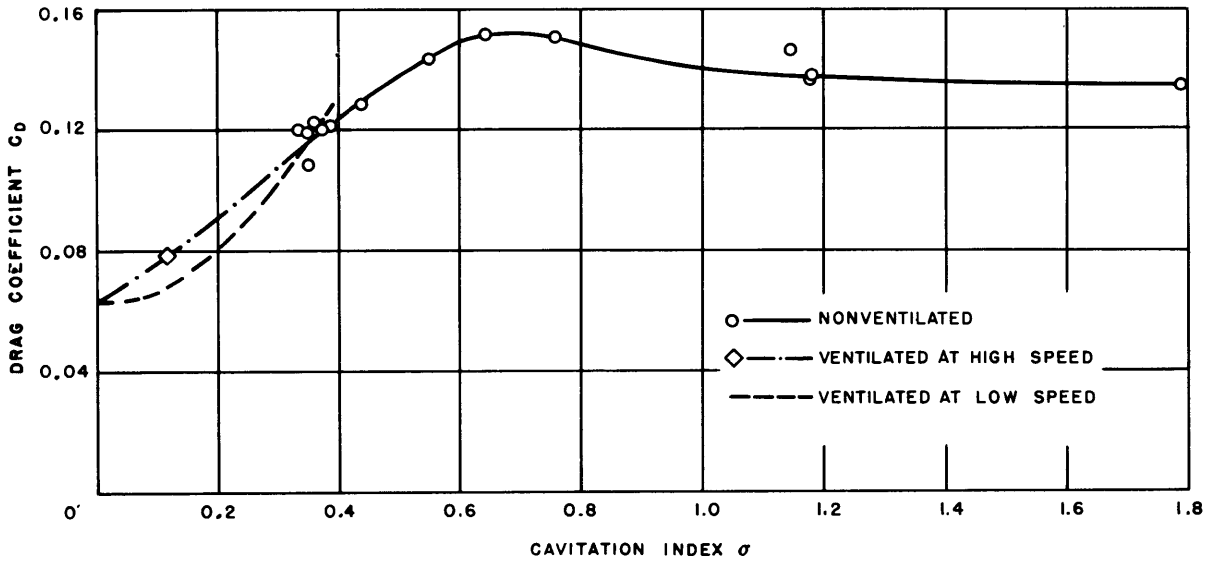

Figure 13a – 11-Degree Angle of Attack

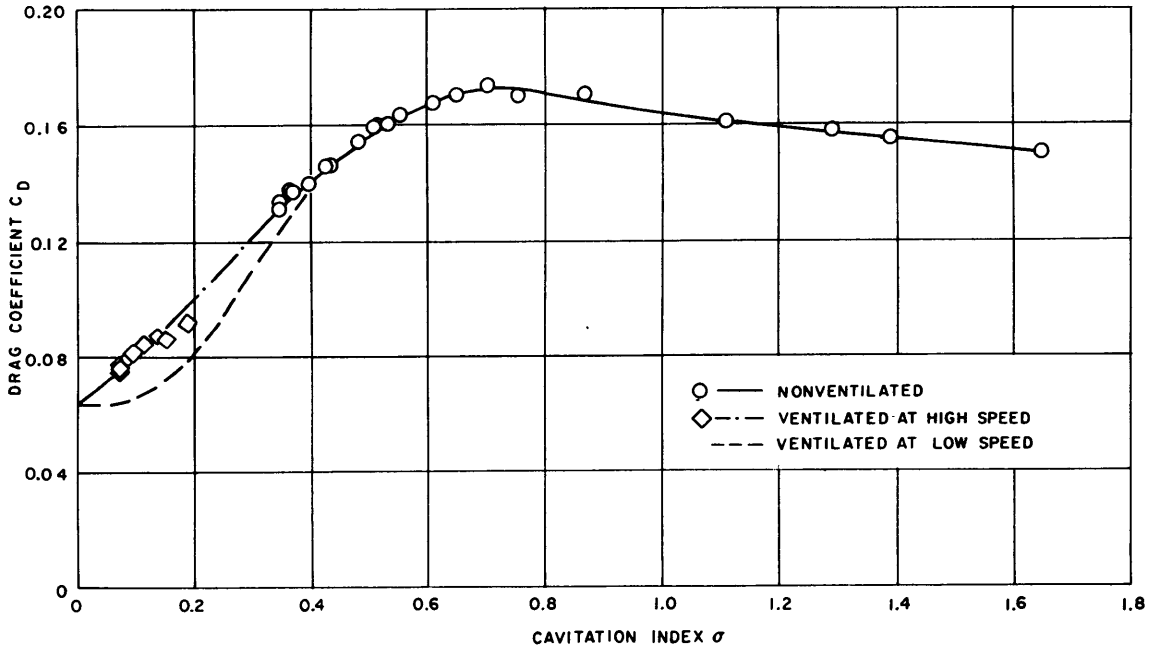

Figure 13b – 12-Degree Angle of Attack

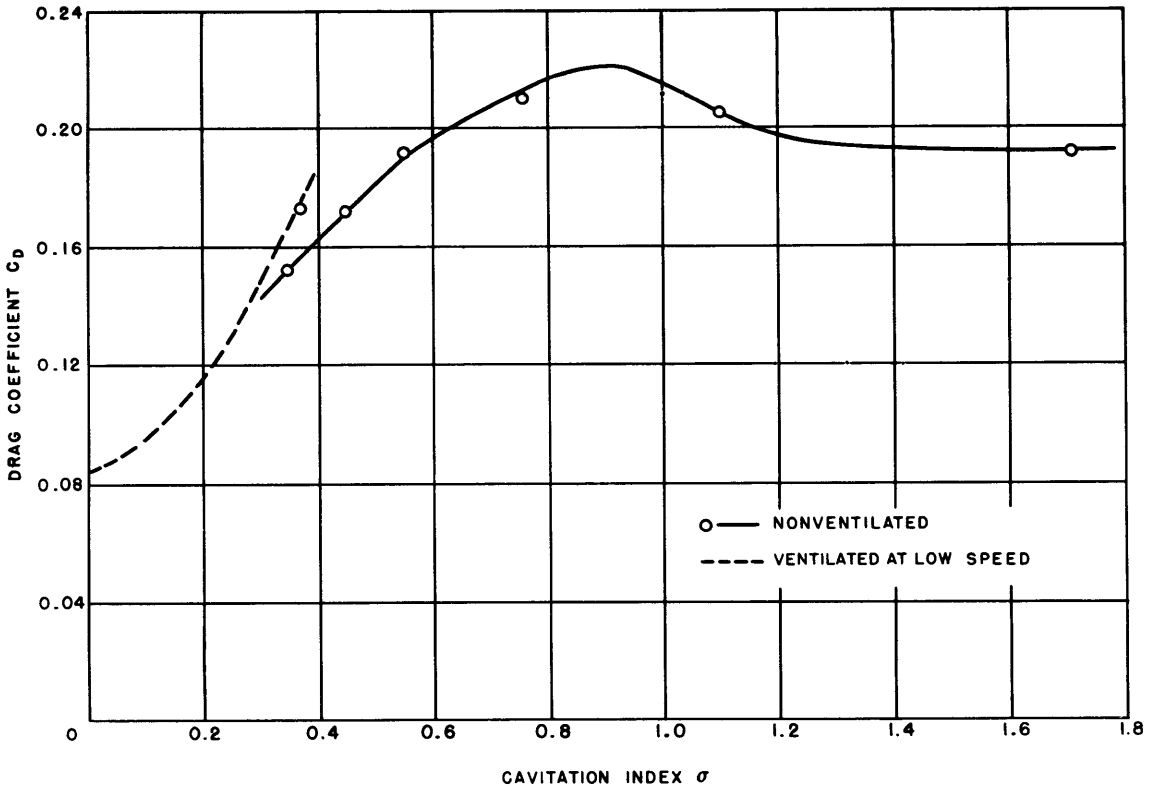

Figure 13c — 14-Degree Angle of Attack

against the effective cavitation number σ_{nv}. The curve of σ_c/σ_{nv} has been faired to a value of zero at $K_v = 0.19$ for the reasons discussed above for low-speed ventilation. The validity of this procedure is not confirmed here since at the angles of attack reported, it was not possible to supply enough air to reach $K_v = 0.19$ in the supercavitating speed range. However, tests with other hydrofoils, not reported here for lack of valid cavity pressure measurements, indicate that the values of C_L and C_D for full ventilation are equal for high-speed and low-speed ventilation. This fairing does not affect any of the test points reported here but is shown to indicate the recommended procedure.

Observation of Figures 12a, 12b, 13a, and 13b shows a discrepancy between the curves of C_L and C_D versus σ as obtained from the high-speed and low-speed ventilated tests. At present, it cannot be stated which is more correct. The low-speed ventilated results may be better for low values of σ (high values of K_v). However, the high-speed ventilated results yield a curve whose shape appears more reasonable. The possibility that low-speed ventilation represents a different physical phenomenon than supercavitation must be studied.

Figure 14 – Variation of Lift and Drag Coefficient with Ventilation Index for the Ventilated Hydrofoil at Subcavitating Speeds

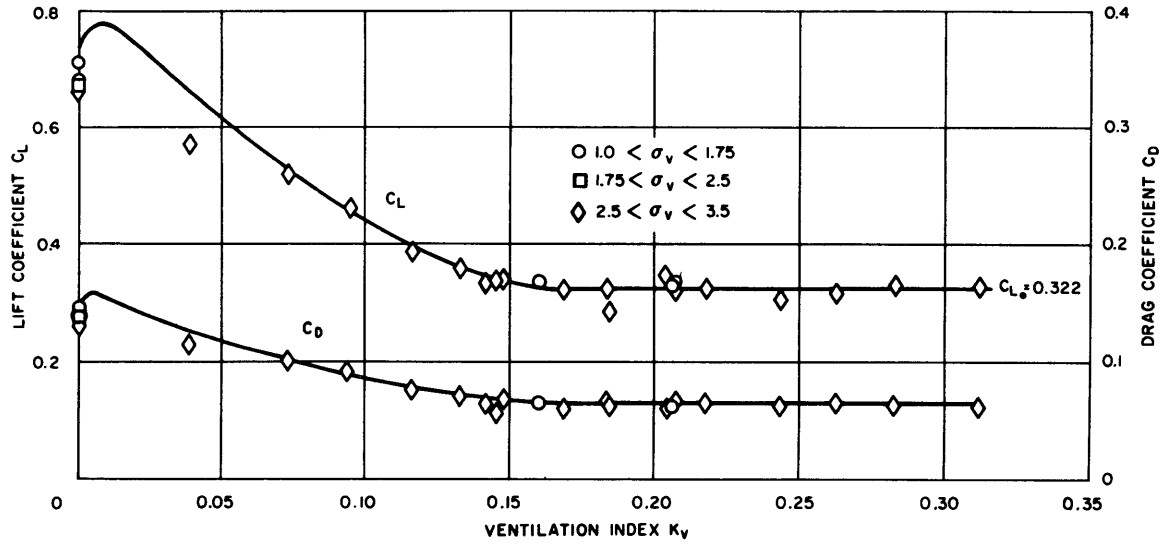

Figure 14a – 11-Degree Angle of Attack

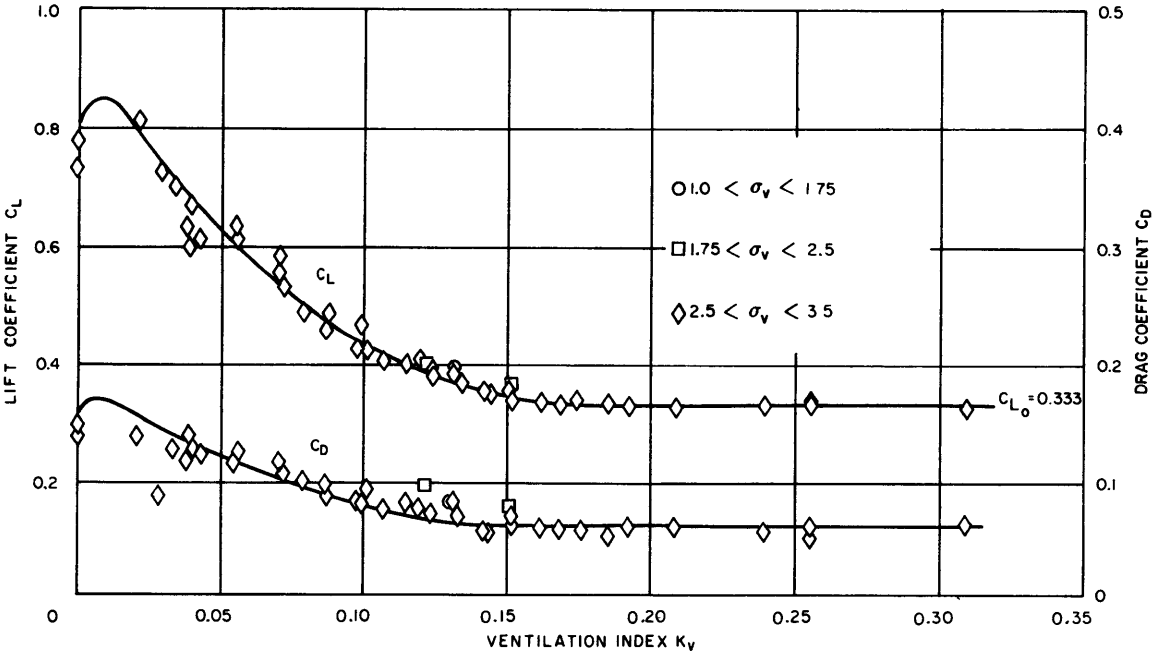

Figure 14b – 12-Degree Angle of Attack

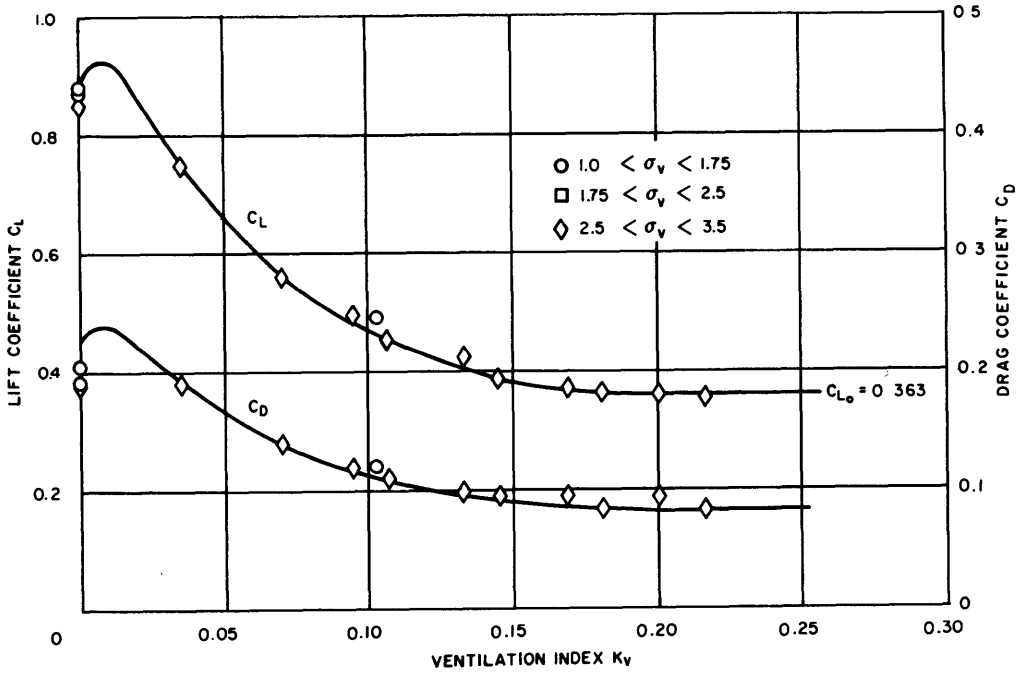

Figure 14c — 14-Degree Angle of Attack

SUMMARY AND CONCLUSIONS

The lack of agreement between the measured cavity pressure and vapor pressure requires further investigation. Tests not included in this report indicate that the measured pressure inside the cavity varies considerably with the air content of test water. So far these findings are only of qualitative nature. Further investigation is planned to determine a definite relation between cavity pressure and air content of water. The water of the towing basin, where the tests reported herein were conducted, has a relatively constant air content very close to saturation. Air content is therefore not expected to be a variable in the results reported in this paper.

With ventilation at either high or low speeds, it has been shown that C_L reaches a limiting value appropriate to zero cavitation number. However, the cavity pressure reaches a limit which is approximately equal to the atmospheric pressure instead of reaching the ambient pressure, which is higher than atmospheric pressure by an amount equal to the head of the water above the foil.

Analysis of the results for high- and low-speed ventilation yield different curves. It seems likely that the high-speed results are more nearly correct. Possibly the mechanism of low-speed ventilation is sufficiently different from supercavitating flow to cause a different

behavior with respect to cavitation number although the same limiting value of C_L is reached. This question will be investigated further.

ACKNOWLEDGMENTS

The authors wish to express their appreciation to Mr. Willard Roundy for his assistance in the instrumentation and testing of the hydrofoil and to many others at the Model Basin who assisted in various areas of work.

REFERENCES

1. Johnson, V.E. Jr., "Theoretical Determination of Low-Drag Supercavitating Hydrofoils and Their Two-Dimensional Characteristics at Zero Cavitation Number," National Advisory Committee for Aeronautics RM L57G11a (1957).

2. Christopher, K.W. and Johnson, V.E. Jr., "Experimental Investigation of Two Low-Drag Supercavitating Hydrofoils at Speeds up to 200 Feet Per Second," National Aeronautics and Space Administration TN D-436 (Aug 1960).

3. Eisenberg, P. and Pond, H.L., "Water Tunnel Investigations of Steady State Cavities," David Taylor Model Basin Report No. 668 (Oct 1948).

4. Kermeen, R.W., "Water Tunnel Tests of NACA 4412 and Walchner Profile 7 Hydrofoils in Noncavitating and Cavitating Glows," California Institute of Technology Report No. 47-5 (Feb 1956).

5. Silberman, E. and Song, C.S., "Instability of Ventilated Cavities," Journal of Ship Research, Vol. 5, No. 1 (Jun 1961).

INITIAL DISTRIBUTION

Copies

12 CHBUSHIPS
- 3 Tech Lib (Code 210L)
- 1 Ship Silencing (Code 345)
- 1 Ship Design (Code 410)
- 3 Prelim Des (Code 420)
- 1 Sci & Res (Code 442)
- 1 Boats & Small Craft (Code 449)
- 1 Hull Mach (Code 632)
- 1 Lab Mgt (Code 320)

2 CHONR
- 2 Fluid Dynamics (Code 438)

2 CHBUWEPS
- 1 Aero & Hydro (Code RAAD-3)
- 1 Dir for Systems Analysis (Code R-52)

1 CNO, Op-725

1 CDR, USNOTS, Pasadena
- 1 Oceanic Research Gp

1 DIR, Langley Res Ctr, NASA
Attn: Mr. John B. Parkinson

26 DTMB High Speed Phenomena Div
Langley Field,
Attn: Mr. R.E. Olsen

2 California Institute of Technology, Pasadena
Attn: Hydrodynamics Lab

1 DIR, Davidson Laboratory
Stevens Inst of Tech

1 Dept of NAME, MIT

1 DIR, St. Anthony Falls Hydraulic Lab

1 DIR, Iowa Inst of Hydraulic Research

1 Stanford University
Attn: Dr. B. Perry

1 University of California
Inst of Engineering Res, Berkely
Attn: Prof. R. Paulling

Copies

1 Boeing Airplane Company
Aero-Space Div, Box 3707, Seattle
Attn: R. E. Bateman
Internal Mail Sta 46-74

1 Hydrodynamic Research Lab
Convair Div, General Dyn Corp, San Diego

2 Grumman Aircraft Engineering Corp
Marine Engineering Section, Bethpage

1 Pres., Hydronautics, Inc.
Pindell School Road, Laurel, Md.

1 Technical Research Group, Inc.
2 Aerial Way, Syosset, N.Y.

1 Aerojet General Corp., Azusa
Attn: Mr. J. Levy

1 Lockheed Aircraft Corp, Hydrodynamic Gp,
Sunnyvale, California
Attn: Mr. R. W. Kermeen

1 Oceanics, Inc.,
114 East 40th St, N.Y. 16, N.Y.
Attn: Dr. Paul Kaplan

1 FMC Corporation
Ordnance Div., P. O. Box 367, San Jose

1 Lycoming Division, AVCO Corp.
550 South Main Street, Stratford, Conn.